Visualizing Diffusion Tensor MR Images Using Streamtubes and Streamsurfaces

Song Zhang, Charlie Curry, Daniel S Morris, David H Laidlaw, Brown University Computer Science, Providence, RI

1. Introduction

In biological tissue, water is ubiquitous and constantly in motion. This motion of water inside biological tissue is called diffusion. Water usually diffuses at different rates both in different locations and along different directions at one location. The difference of diffusion rates at one location is called anisotropy. The following pictures show three types of diffusion illustrated by the ellipsoids. The ellipsoid would be regarded as the shape that the water will diffuse into from one point after a short period of time. Thus it is a natural icon for diffusion information.

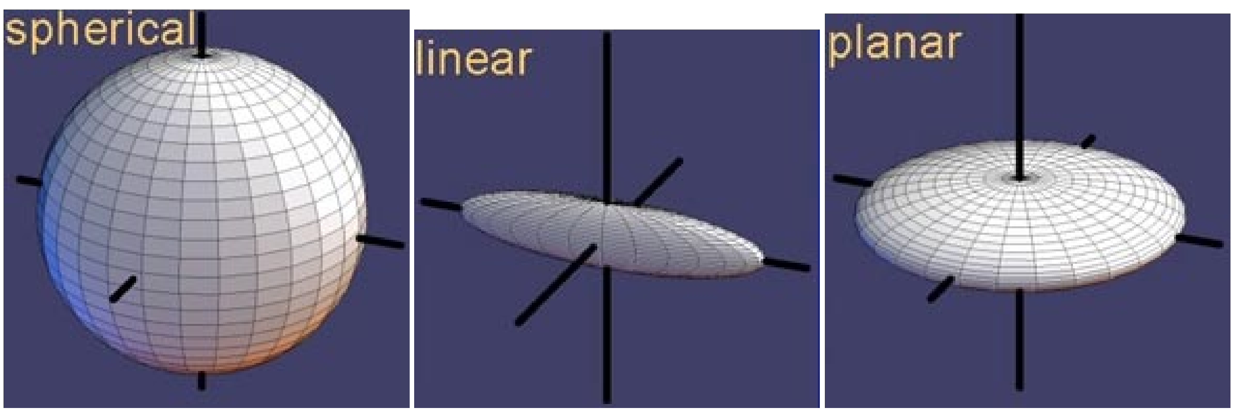

The diffusion of water is constrained by, and correlated with, micro-structure in the biological tissue. By visualizing diffusion information, we can elucidate the connectivity and micro-structural detail.
With MRI technology, diffusion information can be measured *in vivo* from biological tissues, producing a three-dimensional, second-order tensor field. This tensor field consists of a description of the diffusion information at every sample point in the three-dimensional volume.
In this project, we produce images from the three-dimensional diffusion tensor fields that illustrate the connectivity and other micro-structural information in the nervous system; we provide the user with interactivity so that he/she can explore the image from different angles and distances; we also put anatomical landmarks in the image which is proved to be essential in understanding the images.

2. Related Work: Ellipsoids in 2D

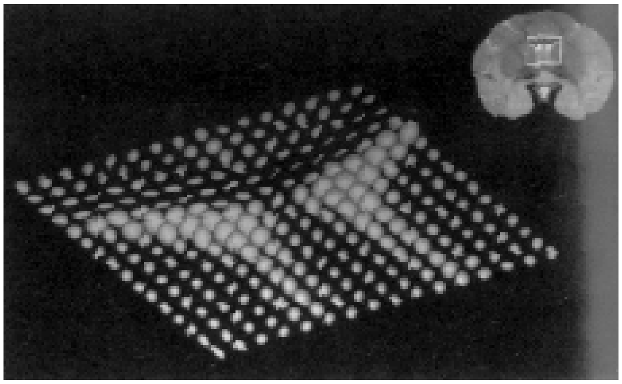

a

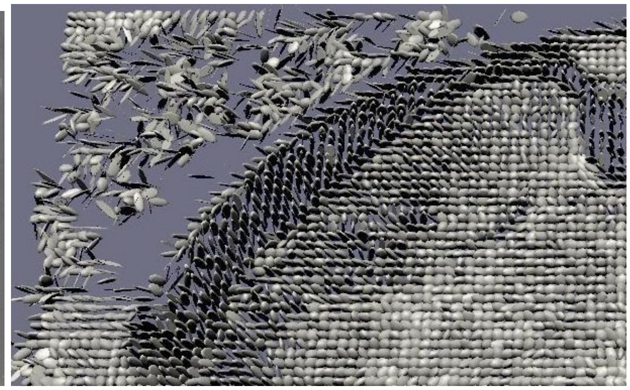

b

Pierpaoli *et al* use arrays of ellipsoids[Pierpaoli and Basser, 1996] to represent a two-dimensional diffusion tensor field(Figure a). A diffusion tensor matrix is symmetric and has positive eigenvalues. These special properties make an ellipsoid a natural geometric representation of the diffusion tensor. Each axis of the ellipsoid represents one eigenvector and its corresponding eigenvalue. Laidlaw *et al* normalized the size of the ellipsoid to give a more continuous visual appearance [Laidlaw et al., 1998](Figure b).

3. Related Work: Brushstrokes in 2D

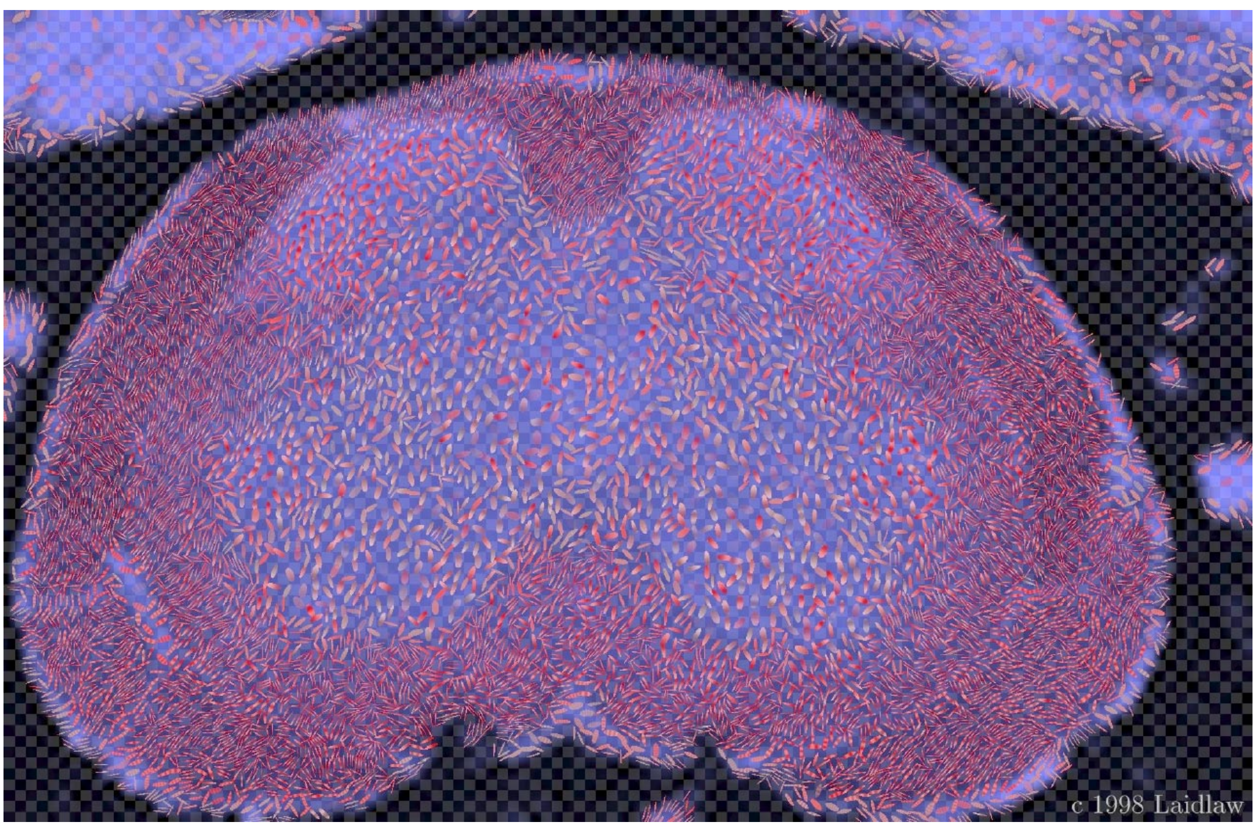

Laidlaw *et al* [Laidlaw et al., 1998] borrow concepts from oil painting. Two-dimensional brush strokes are used to represent different aspects of the diffusion tensors. The information is also classified and visualized in different layers such as the underpainting, checkerboard layer, and stroke layer.

4. Geometric representation in 3D

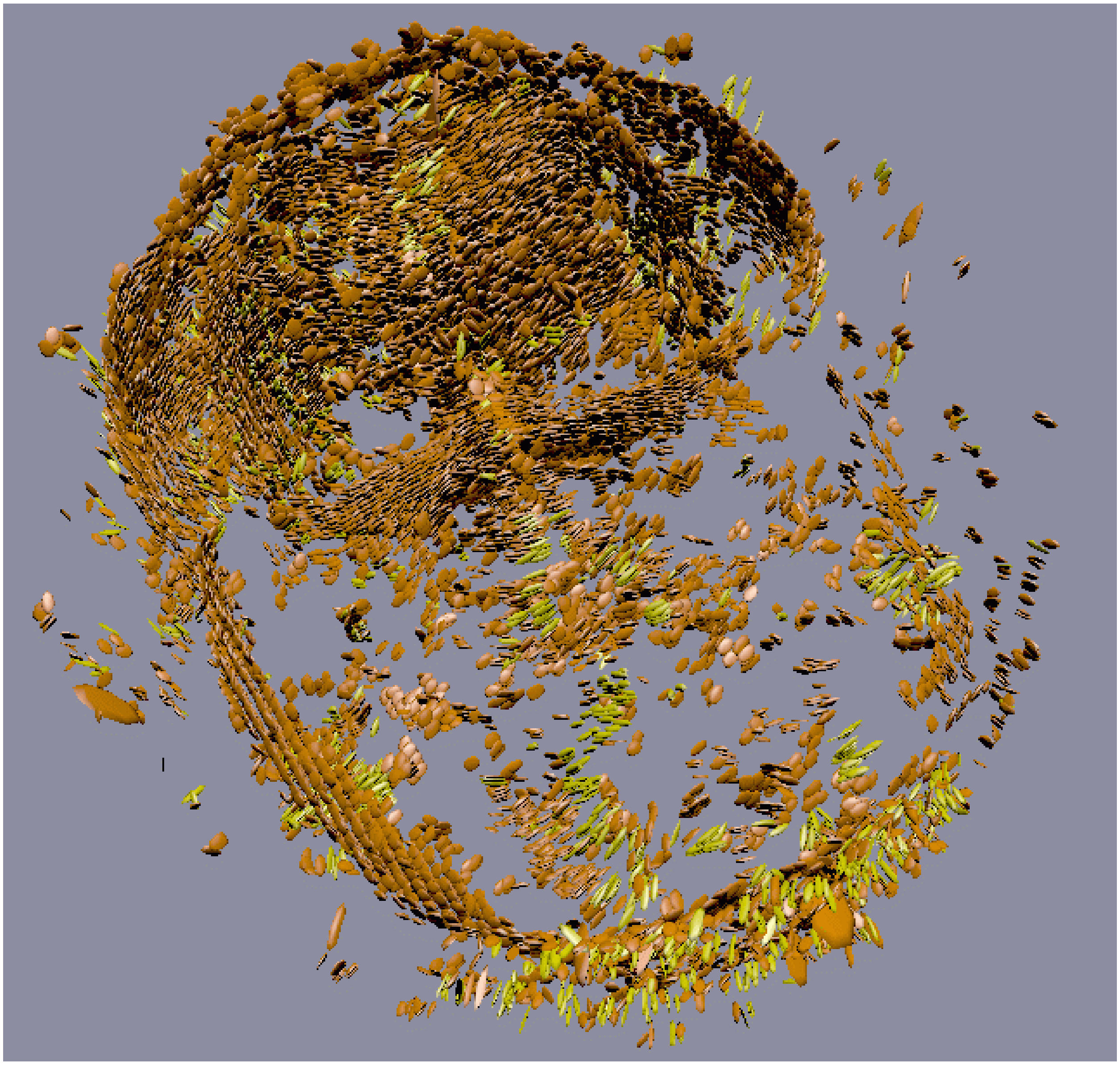

There are two limitations of ellipsoids methods when applied to a three-dimensional dataset. First, visualizing every sample point in the three-dimensional dataset, only the outermost layer of the dataset can be displayed on the screen. The internal data points will be blocked. Second, continuity inherent in biological tissues will not be properly represented in the final image. For example, the neural fibers in the brain that connect different anatomical regions would be difficult to locate within an array of ellipsoids.

Similar problems arise when we try to apply the brushstrokes method to visualize a three-dimensional diffusion tensor field.

5. Related Work: 3D Volume Rendering

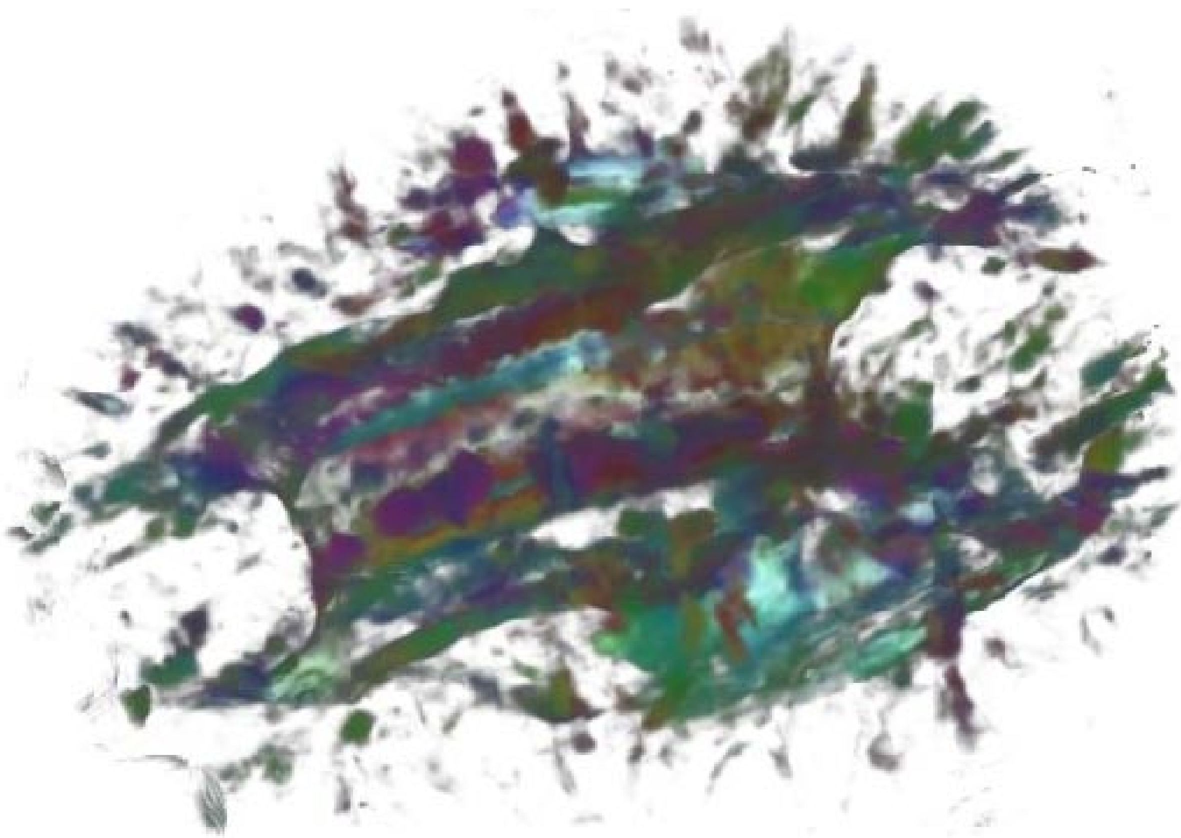

Kindlmann *et al* [Kindlmann and Weinstein, 1999] take a volume rendering approach to the problem. The philosophy behind this method is to display only some of the information, but display that information densely within a volume. The "hue-ball" and a "barycentric map" assign color and opacity to each location in the dataset based on the properties of the diffusion tensor information. Although low opacity is assigned to unimportant data to avoid visual cluttering, in many cases there are a number of important data points along the direction of one ray. The compression of all these points into a single pixel makes it difficult for a viewer to extract precise positional information from the final image. This makes it difficult to pick out the path of a certain fibrous structure from its neighborhood. Also, a lack of interactivity limits a user's understanding of the image.

6. Our method—Streamtubes and streamsurfaces

Our solution is to distinguish between linear and planar anisotropy regions, and employ streamtubes and streamsurfaces to visualize these two types of regions, respectively.

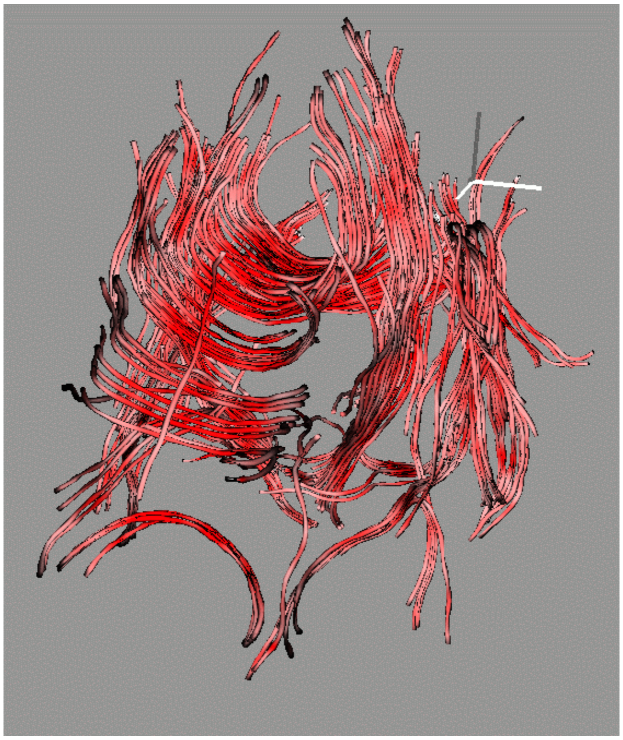

Streamtubes

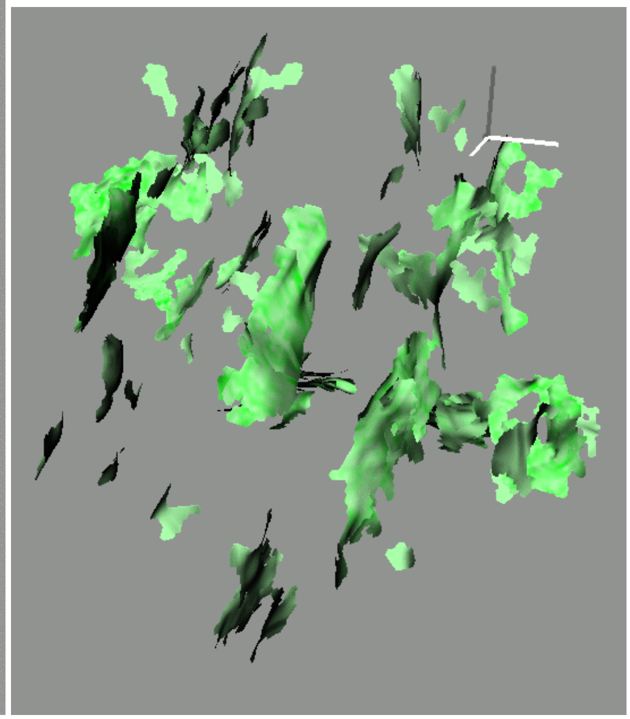

Streamsurfaces

The streamtubes represent linear anisotropy region. The trajectory sweeps along the major vector field, and the cross-section shape is an ellipse representing the other two eigenvectors. We normalize the length of the medium eigenvector to a constant value so that the size of the streamtube is predictable, while the ratio between medium and minor eigenvalues remains intact. The color of the streamtube is related to the linear anisotropy value.

The streamsurfaces represent planar anisotropy region. It is an approximation of the integral surface in both the major eigenvector field and the medium eigenvector field. Colors are mapped to the surfaces to represent the planar anisotropy value.

8. Anatomical Landmarks

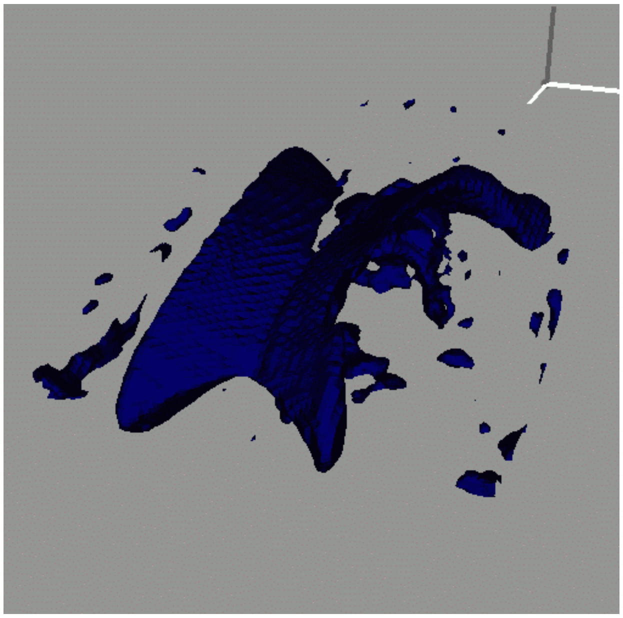

Ventricle

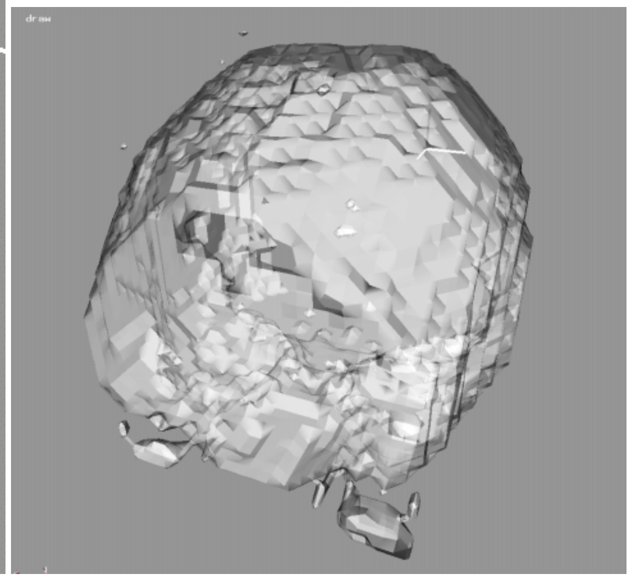

Inside Skull Surface

Based on the feedback from preliminary results, we found that biologists tended to explore the image more efficiently if they can easily identify some obvious large structures that they are familiar with in the image. For example, if they are looking at an image of the human brain, knowing the position of the skull, eyes, and ventricles makes it easier to find structures in the rich information provided by our diffusion tensor visualization method. For this reason, we provided anatomical landmarks in our image. These landmarks are created by generating isosurfaces from T2-weighted images using AVS[Upson et al., 1989].

7. Geometry selection

Initially, we generate streamtubes and streamsurfaces so that every voxel that has linear anisotropy or planar anisotropy will be run through by a streamtube or a streamsurface. That will give us a dense set of geometries. Visualizing them all is not only expensive, but also undesirable, as the inclusion of too many streamtubes in the scene will generate visual cluttering. So we have to decide which ones should be selected and visualized.

For streamtubes, we use three criteria to measure their importance:

- *Length*—Streamtubes shorter than a given threshold are removed. Short streamtubes could be the result of either noise or reflection of short linear structures. For our purpose, short structures are less significant than long ones.
- *Average linear anisotropy*—By averaging the linear anisotropies at each point on a streamtube, we can get an idea of whether the streamtube passes through a region of high anisotropy. If so, it is assumed to represent a preferred direction of diffusion, and it is kept for visualization.
- *Similarity to previously selected streamtubes*—We drop the streamtubes that are too "close" to selected ones, thus removing the "duplicates". We define the distance between two curves to be:

$$D=\begin{cases} 0 & \text{if } \int_{s_0}^{s_1} \max(\operatorname{sgn}(\operatorname{dist}(s)-T_l),0)\,\mathrm{d}s = 0 \\ \dfrac{\int_{s_0}^{s_1} \max(\operatorname{dist}(s)-t,0)\,\mathrm{d}s}{\int_{s_0}^{s_1} \max(\operatorname{sgn}(\operatorname{dist}(s)-T_l),0)\,\mathrm{d}s} & \text{otherwise} \end{cases}$$

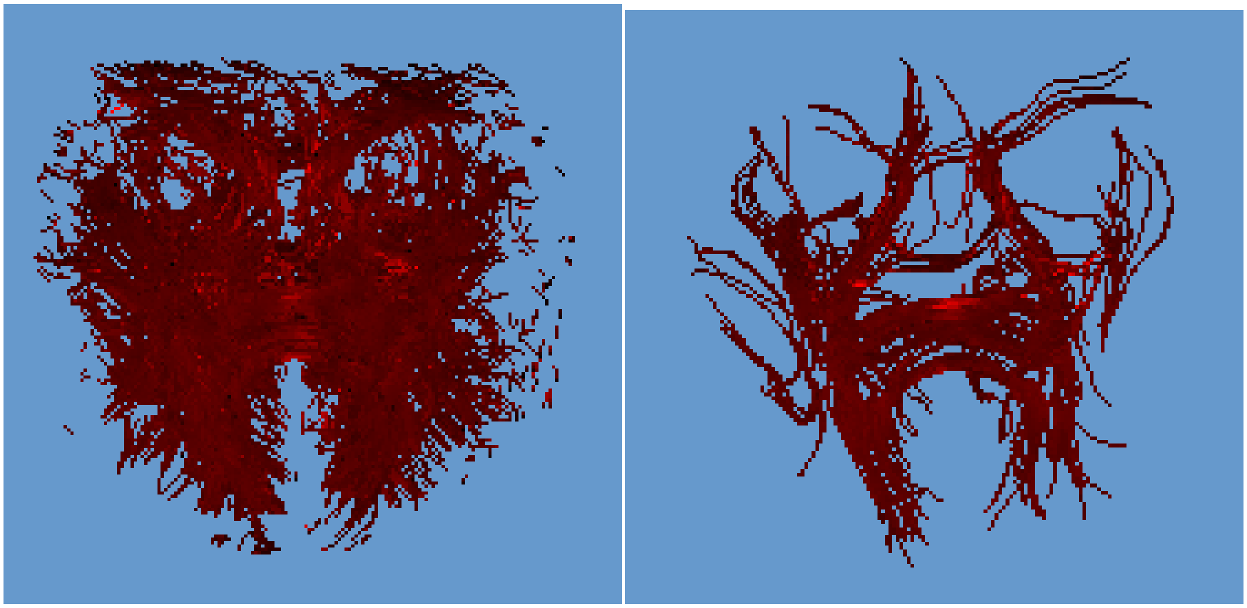

These two pictures show us the original set of streamtube-trajectories, and a selected set of streamtube-trajectories.
Similarly, for streamsurface, we use the size of the streamsurface, average planar anisotropy, and similarity to previously selected streamsurfaces as three criteria to measure their importance.

9. Results

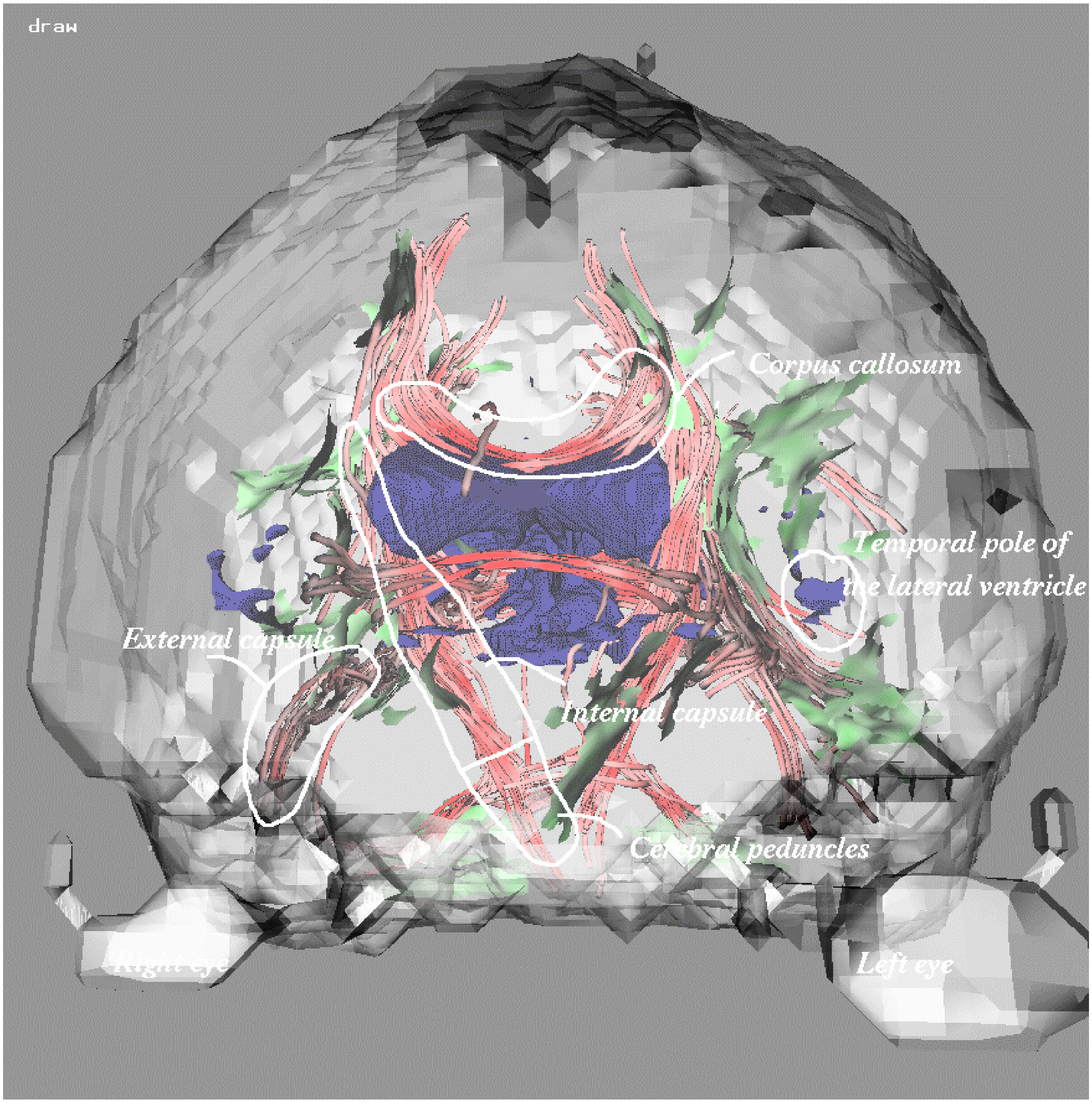

This annotated image shows the human brain from the eye to the top of the head. Through the semi-transparent skull surface, we can see the ventricle (colored blue) in the middle, and the streamtubes and the streamsurfaces in the space.

The parameters used to generate this image are listed in table below:

Streamtube length	$> 26.70\,\mathrm{mm}$
Average linear anisotropy	> 0.40
T_l used in D for streamtubes	$1.34\,\mathrm{mm}$
Distance between lines	$> 44.5\,\mathrm{mm}$
Surface size	$> 7.00\,\mathrm{mm}^2$
Average planar anisotropy	> 0.30
T_s used in D for streamsurfaces	$1.34\,\mathrm{mm}$
Distance between surfaces	$> 8.9\,\mathrm{mm}$

10. Different views of the human brain image

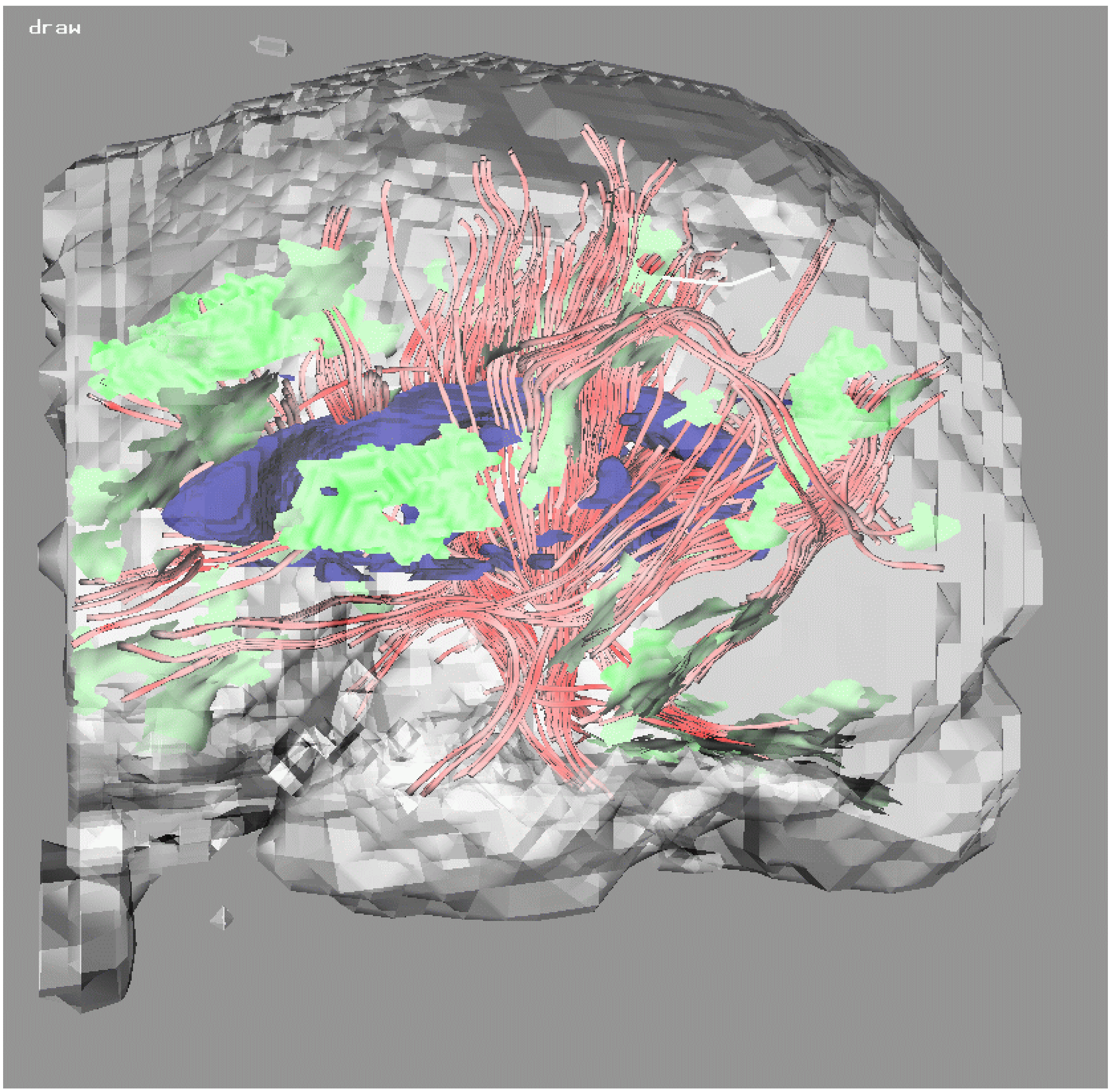

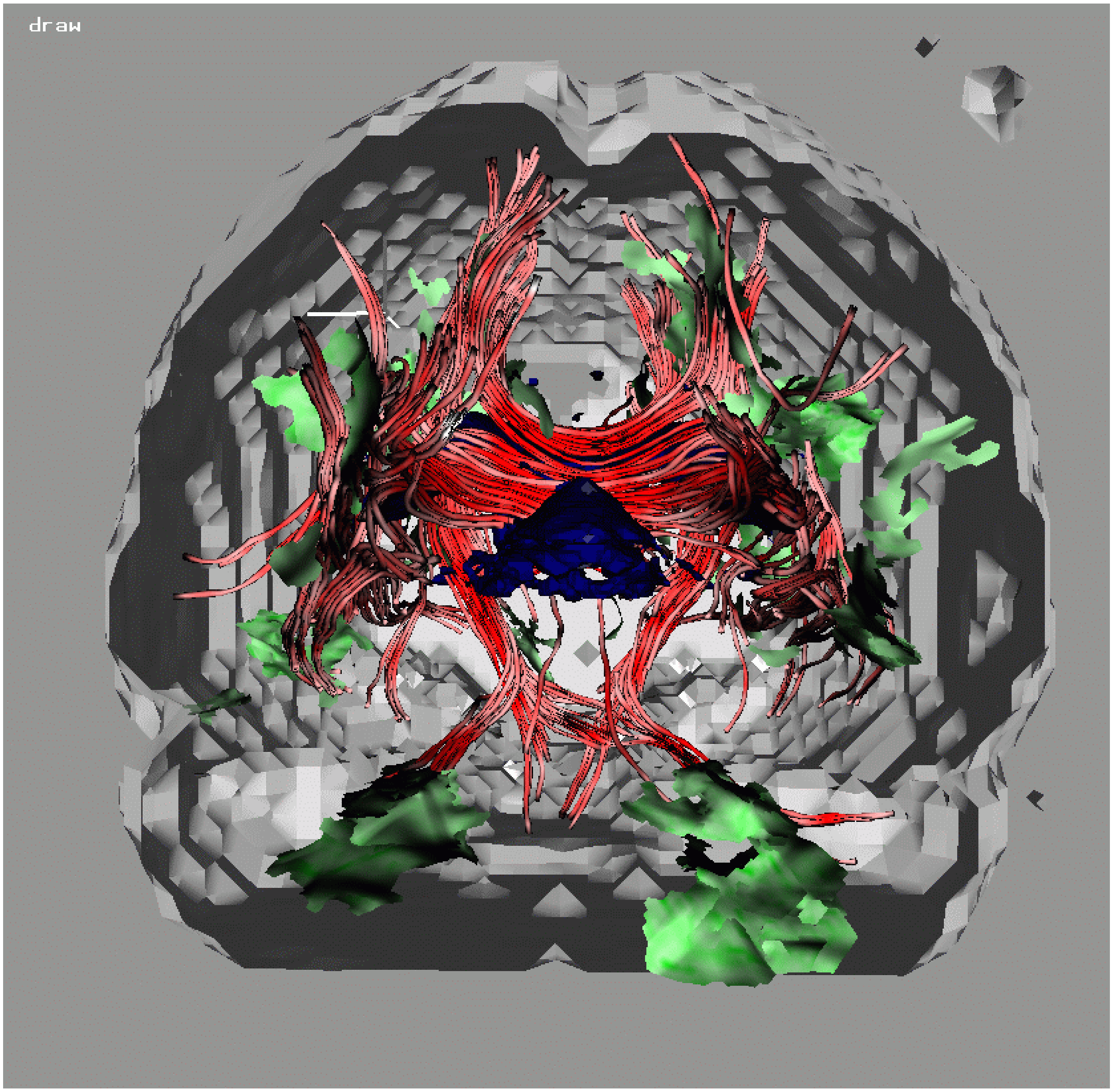
draw

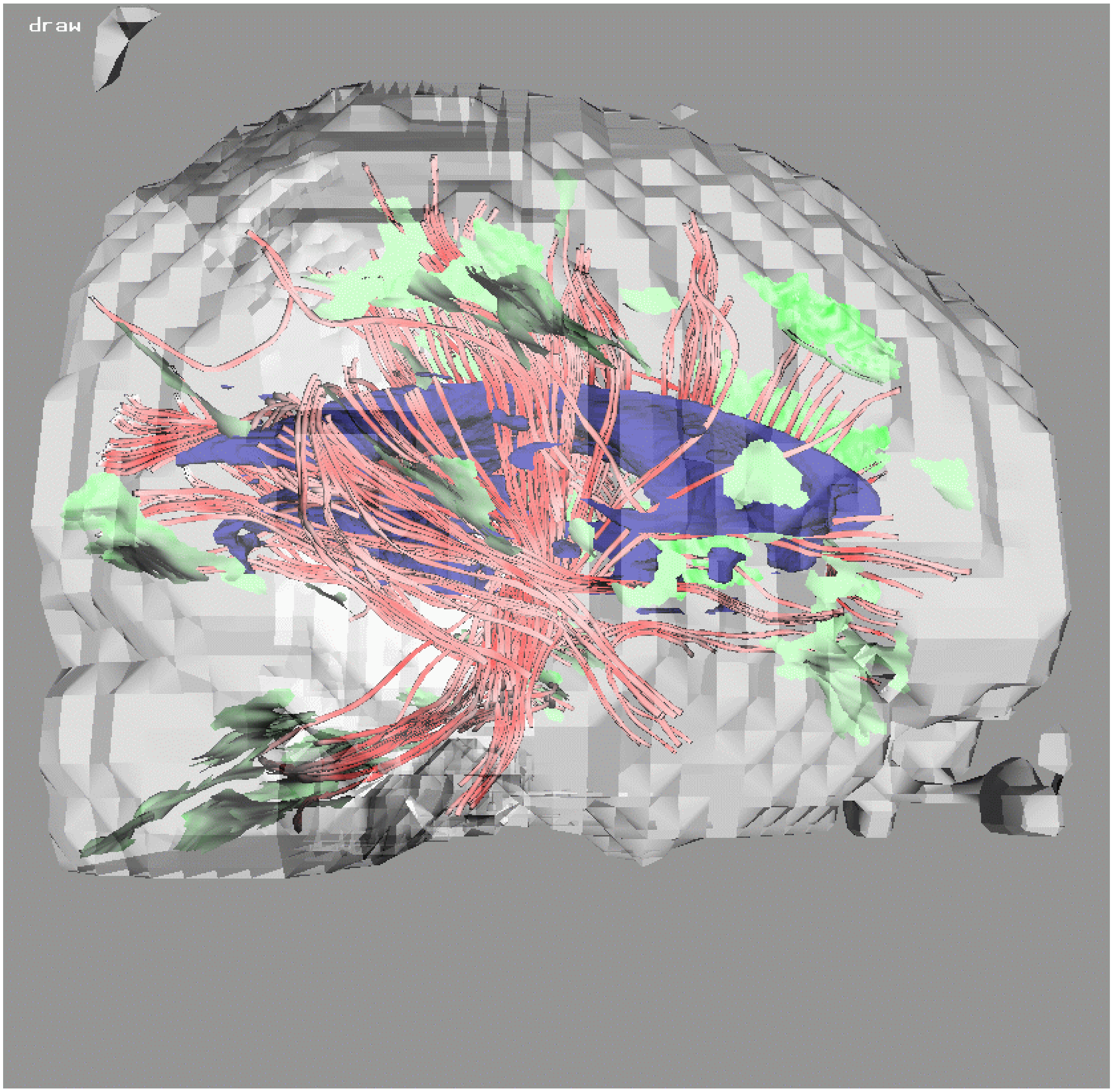
draw

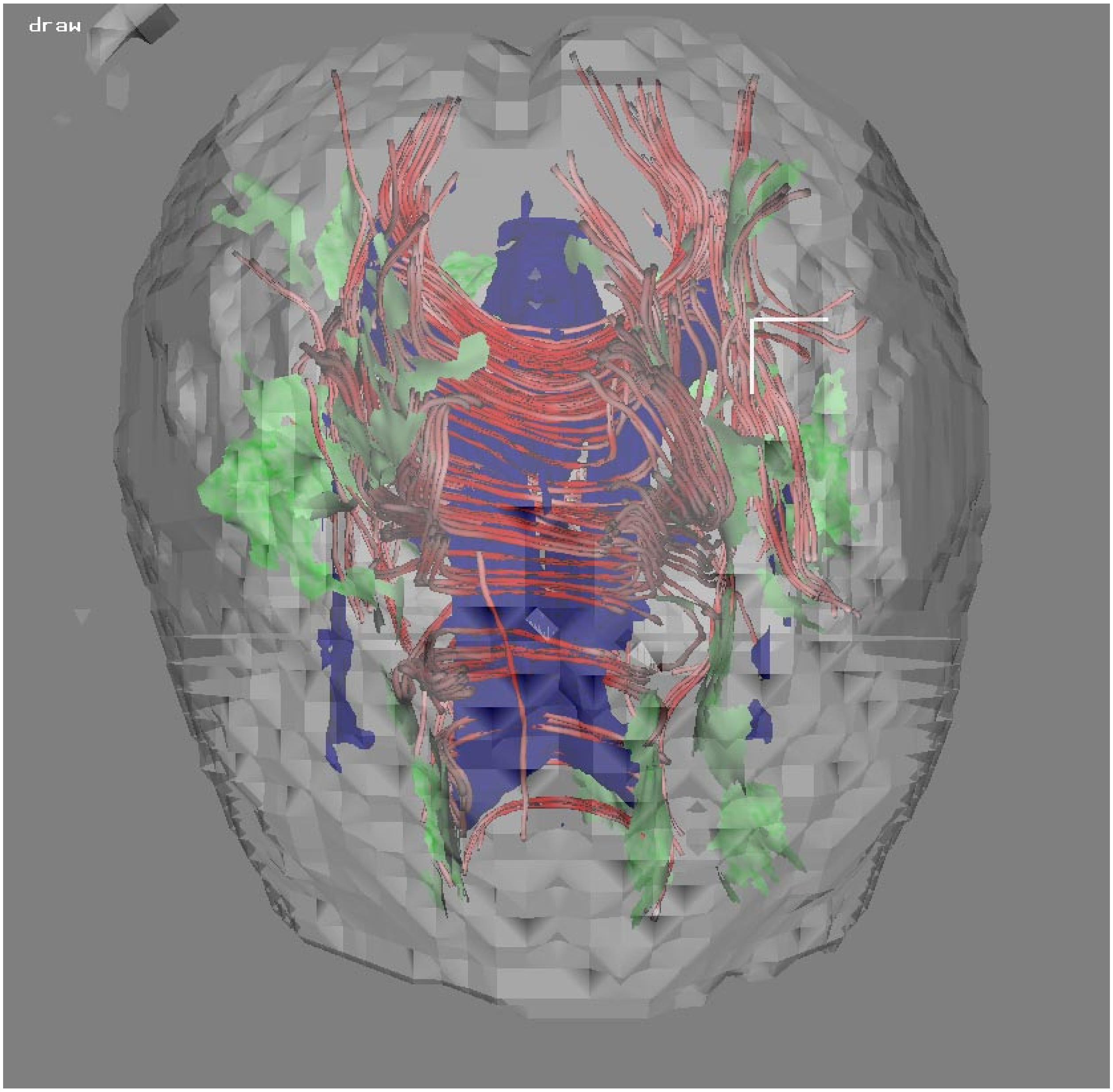

11. Effects of parameters on the final images

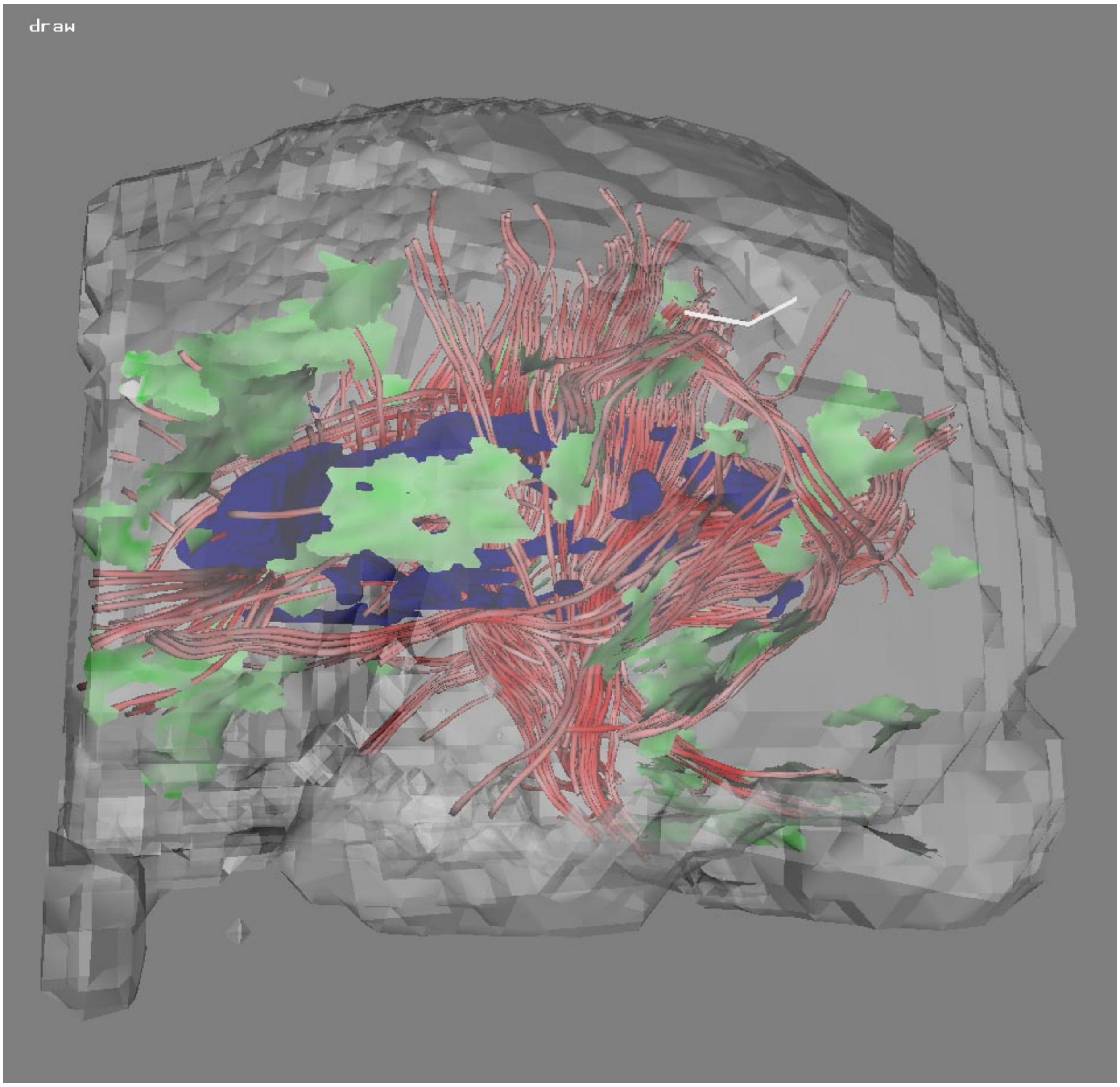

Distance between lines reduced
from $> 44.5\,\mathrm{mm}$ to $> 26.7\,\mathrm{mm}$

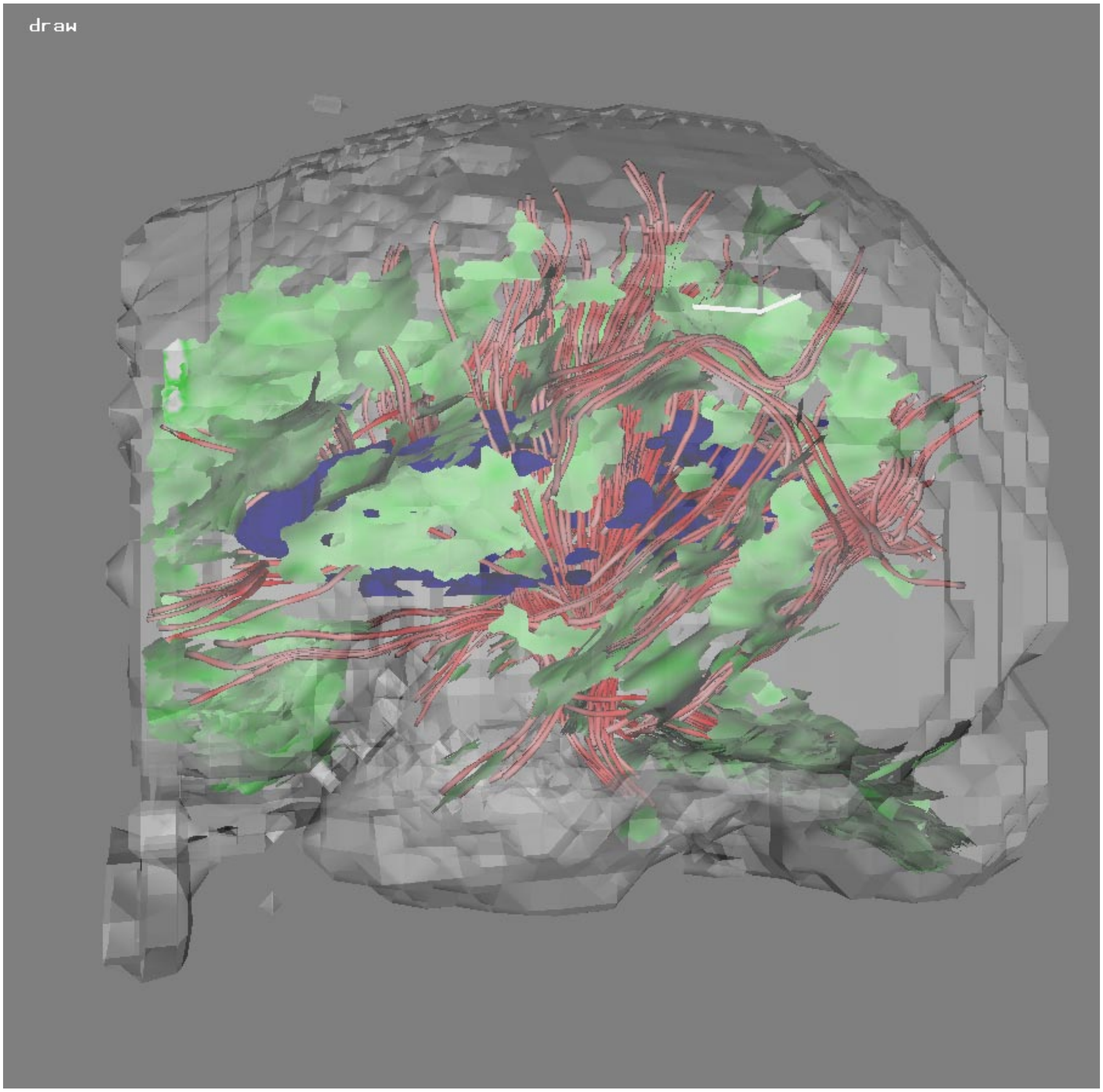

Distance between streamsurfaces reduced from
$> 8.9\,\mathrm{mm}$ to $> 4.5\,\mathrm{mm}$

Lessons

- The geometric models we create show connectivity in the brain
- Anatomical landmarks are essential for understanding these images
- Choosing which parts of the data to represent is a difficult problem

12. Acknowledgment

Thanks to Dr. Susumu at Johns Hopkins University who kindly sent us the human brain dataset and Eric Ahrens for the mouse embryo dataset. Thanks to Eric Ahrens, Russell Jacobs, Seth Ruffins, Rusty Lansford, and David Berson for providing feedback and evaluation on our results. Also thanks to our sponsor, the Human Brain Project.

References

[Cormans et al., 1994] Cormans, J., Luypaert, R., Verhelle, F., Stadnik, T., and Osteaux, M. (1994). A method for myelin fiber orientation mapping using diffusion-weighted mr-images. *MAGNETIC RESONANCE IMAGING*, pages 443–454.

[Delmarcelle and Hesselink, 1992] Delmarcelle, T. and Hesselink, L. (1992). Visualization of second order tensor fields and matrix data. *IEEE Visualization 92 Proceedings*, pages 316–323.

[Kindlmann and Weinstein, 1999] Kindlmann, G. and Weinstein, D. (1999). Hue-balls and lit-tensors for direct volume rendering of diffusion tensor fields. *IEEE Visualization 99 Proceedings*.

[Laidlaw et al., 1998] Laidlaw, D. H., Ahrens, E. T., Kremers, D., Avalos, M. J., Jacobs, R. E., and Readhead, C. (1998). isualizing diffusion tensor images of the mouse spinal cord. *IEEE Visualization 98 Proceedings*, pages 127–134.

[Pierpaoli and Basser, 1996] Pierpaoli, C. and Basser, P. (1996). Toward a quantitative assessment of diffusion anisotropy. *Magnetic Resonance Magazine*, pages 893–906.

[Upson et al., 1989] Upson, C., Faulhaber, T., Jr., D. K., Laidlaw, D., Schlegel, D., Vroom, J., Gurwitz, R., and van Dam, A. (1989). The application visualization system: A computational environment for scientific visualization. *IEEE Computer Graphics and Applications*, 9:30–42.

[Westin et al., 1997] Westin, C. F., S. Peled, H. G., Kikinis, R., and Jolesz, F. (1997). Geometrical diffusion measures for mri from tensor basis analysis. *Proceedings of ISMRM*.

[Xue et al., 1999] Xue, R., van Zijl, P. C., Crain, B. J., Solaiyappan, M., and Mori, S. (1999). In vivo three-dimensional reconstruction of rat brain axonal projections by diffusion tensor imaging. *Magnetic Resonance in Medicine*, 42.

[Zoeckeler et al., 1996] Zoeckeler, M., Stalling, D., and Hege, H.-C. (1996). Interactive visualization of 3d-vector fields using illuminated streamlines. *IEEE Visualization 96 Proceedings*, pages 107–113.